AAC Accepted Manuscript Posted Online 8 August 2016
Antimicrob. Agents Chemother. doi:10.1128/AAC.01339-16

Discovery of novel oral protein synthesis inhibitors of *Mycobacterium tuberculosis* that target leucyl-tRNA synthetase

***Andrés Palencia[1†], *Xianfeng Li[2]**, Wei Bu[2], Wai Choi[2], Charles Z. Ding[2], Eric E. Easom[2], Lisa Feng[2], Vincent Hernandez[2], Paul Houston[2], Liang Liu[2], Maliwan Meewan[2], Manisha Mohan[2], Fernando L. Rock[2], Holly Sexton[2], Suoming Zhang[2], Yasheen Zhou[2], Baojie Wan[3], Yuehong Wang[3], Scott G. Franzblau[3], Lisa Woolhiser[4], Veronica Gruppo[4], Anne J. Lenaerts[4], Theresa O'Malley[5], Tanya Parish[5], Christopher B. Cooper[6], M. Gerard Waters[6], Zhenkun Ma[6], Thomas R. Ioerger[7], James C. Sacchettini[7], Joaquín Rullas[8], Iñigo Angulo-Barturen[8], Esther Pérez-Herrán[8], Alfonso Mendoza[8], David Barros[8], Stephen Cusack[1], Jacob J. Plattner[2] and **M.R.K. Alley[2#]**

[1]European Molecular Biology Laboratory (EMBL), Grenoble, France
[2]Anacor Pharmaceuticals, Palo Alto, CA, USA
[3]Institute for Tuberculosis Research, University of Illinois at Chicago, Chicago, IL, USA
[4]Mycobacteria Research Laboratories, Department of Microbiology, Immunology and Pathology, Colorado State University, Fort Collins, CO, USA
[5]TB Discovery Research, Infectious Disease Research Institute, Seattle, WA, USA
[6]Global Alliance for TB Drug Development, New York, USA
[7]Department of Biochemistry & Biophysics, Texas A&M University, College Station, TX, USA
[8]Tres Cantos Medicines Development Campus (TCMDC), GlaxoSmithKline (GSK), Tres Cantos, Spain

*Co-first authors
Correspondence should be addressed to M.R.K. Alley (dickon_alley@mac.com)

†Present address: Andrés Palencia, Institut for Advanced Biosciences, Team Host-pathogen interactions & immunity to infection, INSERM U1209, CNRS UMR5309, Université Grenoble Alpes, Grenoble, France

RUNNING TITLE: Antitubercular leucyl-tRNA synthetase inhibitors

ABSTRACT

The recent development and spread of extensively (XDR) and totally resistant (TDR) strains of *Mycobacterium tuberculosis*, highlights the need for new antitubercular drugs. Protein synthesis inhibitors have played an important role in the treatment of tuberculosis (TB) starting with the inclusion of streptomycin in the first combination therapies. Although the parenteral aminoglycosides are a key component in multidrug-resistant (MDR) TB therapy, the oxazolidinone, linezolid, is the only orally available protein synthesis inhibitor that is effective against TB. Herein, we show that small molecule inhibitors of aminoacyl-tRNA synthetases (AARS), known to be excellent antibacterial protein synthesis targets, can be designed that are orally bioavailable and effective against *M. tuberculosis* in TB mouse infection models. We applied the oxaborole tRNA trapping (OBORT) mechanism, which was first developed to target fungal cytoplasmic leucyl-tRNA synthetase (LeuRS), to *M. tuberculosis* LeuRS. X-ray crystallography was used to guide design of LeuRS inhibitors that have good biochemical potency and excellent whole cell activity against *M. tuberculosis*. Importantly, their good oral bioavailability translates into *in vivo* efficacy in both the acute and chronic mouse models of TB with comparable potency to the frontline drug isoniazid.

51 **INTRODUCTION**

52 The aminoacyl-tRNA synthetases (AARS) are a family of essential enzymes that are
53 required for protein synthesis in all cells (38). Although various family members have been
54 targeted for the design of novel antibacterial (37) only the isoleucyl-tRNA synthetase
55 inhibitor, mupirocin, is an FDA-approved antibiotic (36). However, mupirocin is only
56 approved for the topical treatment of staphylococcal and streptococcal skin infections (36)
57 and *M. tuberculosis* is naturally resistant to this agent (31). Leucyl-tRNA synthetase
58 (LeuRS) is a class I AARS that has two active sites separated by a distance of 30 Å; a
59 synthetic site that aminoacylates $tRNA^{Leu}$ and an editing site that ensures the fidelity of
60 translation by a proofreading mechanism (7, 10, 19, 26). Recently boron-containing
61 compounds known as oxaboroles have been shown to inhibit LeuRS by the oxaborole tRNA
62 trapping (OBORT) mechanism (29), which exploits the ability of the boron atom to bond to
63 the cis-diols of the 3´-terminal adenosine nucleotide, Ade76, of $tRNA^{Leu}$. The resulting
64 covalent adduct traps the 3´-end of $tRNA^{Leu}$ in the editing site in a non-productive complex,
65 inhibiting leucylation and thereby protein synthesis (29). Here we report the discovery of
66 novel 3-aminomethyl derivatives that have potent antitubercular activity.
67

MATERIALS AND METHODS

Chemical Synthesis. Starting materials used were either available from commercial sources or prepared according to literature procedures and had experimental data in accordance with those reported. The syntheses of the compounds are described in detail in the Supplementary Material.

Expression, purification and crystallization of *M. tuberculosis* LeuRS editing domain. A DNA fragment coding for the region G309 to I513 of *M. tuberculosis* LeuRS (Uniprot P67510) was cloned into pETM-11 using the *NcoI* and *XdeI* restriction sites (EMBL). The protein containing an N-terminal six-histidine tag was prepared and purified following a similar protocol as for the *E. coli* LeuRS (26), except that the nickel affinity chromatography was conducted at pH 8.0. Protein was stored in buffer comprising 20 mM Tris-HCl (pH 7.4), 100 mM NaCl, 5 mM $MgCl_2$ and 5 mM 2-mercaptoethanol. Crystallization was performed at 20°C by the hanging drop vapor diffusion method. The solutions for the ternary complexes were prepared with 10 mg/mL LeuRS, 5 mM AMP and 1 mM of the corresponding benzoxaborole compound (provided by Anacor Pharmaceuticals, Palo Alto, CA). Initial crystals were obtained at 15 mg/mL LeuRS, 5 mM AMP and 1 mM of the corresponding benzoxaborole compound (provided by Anacor Pharmaceuticals, Palo Alto, CA). Crystals were obtained by mixing 2 µL of this solution with 2 µL of reservoir solution containing 0.1 M Bis-TRIS (pH 5.5), 22% (w/v) PEG 10000 and 0.2 M ammonium acetate. Quality and size of final diffracting crystal was improved by decreasing LeuRS concentration to 10 mg/mL and PEG 10000 to 17% (w/v). The crystals were frozen directly in liquid nitrogen in the mother liquor containing 15% (v/v) ethylene glycol as a cryoprotectant.

Structure determination and refinement. All diffraction data sets were collected at the European Synchrotron Radiation Facility (ESRF, Grenoble, France). Data were integrated and scaled with the XDS suite (15). Further data analysis was performed with the CCP4 suite (3). The structure of the LeuRS:AMP-compound 6 complex was initially solved by molecular replacement with PHASER (22) using the *E. coli* LeuRS editing domain structure(20) (PDB 2AJG) as a model. The model was improved by automatic building using ARP-wARP (28) and manual adjustments were made with COOT (9). The structures of the complexes with the compounds 14 and 16 were solved using the editing domain of *M. tuberculosis* LeuRS (described above) as a model. All models were refined using REFMAC5 with anisotropic B-factors. Structure quality was analyzed with MOLPROBITY(4) (http://molprobity.biochem.duke.edu/) and showed all residues in allowed regions (with 95.1-

Antimicrobial Agents and Chemotherapy

98.0% of residues in favored regions) for the different models. Figures were drawn with PYMOL (http://www.pymol.org/).

Aminoacylation assay. An N-terminal six histidine-tagged LeuRS from *M. tuberculosis* H37Rv, which was codon-optimized for *E. coli* (GenScript, Piscataway NJ, USA), was over-expressed and purified according to Novagen (Madison, WI, USA) using an E. coli BL21(DE3) T7 RNA polymerase over-expression strain. Experiments were performed in 96-well microtiter plates, using 80 µL reaction mixtures containing 50 mM HEPES-KOH (pH 8.0), 30 mM $MgCl_2$ 30 mM KCl, 13 µM L-[^{14}C]leucine (306 mCi/mmol, Perkin-Elmer), 15 µM total *E. coli* tRNA (Roche, Switzerland), 0.02% (w/v) BSA, 1 mM DTT, 0.2 pM LeuRS and 4 mM ATP at 30^{0}C. Reactions were started by the addition of 4 mM ATP. After 7 minutes, reactions were quenched and tRNA was precipitated by the addition of 50 µL of 10% (w/v) TCA and transferred to 96-well nitrocellulose membrane filter plates (Millipore Multiscreen HTS, MSHAN4B50). Each well was then washed three times with 100 µL of 5% TCA. Filter plates were then dried under a heat lamp and the precipitated L-[^{14}C]leucine $tRNA^{Leu}$ were quantified by liquid scintillation counting using a Wallac MicroBeta Trilux model 1450 liquid scintillation counter (PerkinElmer, Waltham, MA, USA).

IC_{50} determination. To determine the inhibitor concentration, which reduces enzyme activity by 50% (IC_{50}), increasing concentrations of compound inhibitors that covered the IC_{50} value were incubated with LeuRS enzyme, tRNA and L-leucine for 20 minutes. Reactions were initiated by the addition of 4 mM ATP. Reactions were stopped after 7 minutes then precipitated and counted to quantify radioactivity. IC_{50} values were determined using a 4-parameter logistic nonlinear regression model (Graphpad Software Inc. (La Jolla, CA, USA).

Isothermal titration calorimetry (ITC) experiments. ITC experiments were performed at 25^{0}C using an ITC200 system (MicroCal, GE Healthcare). The editing domain protein was dialyzed for 12 hours against the titration buffer (50 mM HEPES-KOH, 30 mM KCl and 30 mM $MgCl_2$, pH 8.0) at 4^{0}C. Protein solutions at 50 µM plus AMP at 10 mM in the calorimetric cell were titrated with the appropriate compound dissolved in dialysis buffer. Compound solutions at 1-5mM plus AMP at 10 mM were incubated at 37°C during 1 hour before titrations. The heat evolved after each ligand injection was obtained from the integral of the calorimetric signal. The resulting binding isotherms were analyzed by nonlinear least-squares fitting of the experimental data to a single site model. Analysis of the data was performed using Microcal Origin software (OriginLab version 7). Experiments were

performed at least twice. The variability in the binding experiments was estimated to be 5% in the binding enthalpy; and 10% in both the binding affinity and the number of sites.

Determination of minimum inhibitory concentration for *M. tuberculosis*. MIC determinations were mainly determined using resazurin (Alamar Blue) as an indicator for cell growth (6) with additional determinations as described by Ollinger *et al* (25).

Selection of *M. smegmatis* ATCC 700084 single-step mutants. Resistant mutants to compound 1 were isolated on Middlebrook 7H10 medium plus 10% (v/v) oleic albumin dextrose catalase (OADC) supplement (Becton Dickinson) containing compound 1 at 4xMIC. Resistance was confirmed by measuring the mutants MIC value essentially as described by Collins *et al* (6).

Selection of *M. tuberculosis* single-step mutants. *M. tuberculosis* mutants resistant to compound 1 and 13 were isolated as described by Ioerger *et al* (14). Mutants were isolated on Middlebrook 7H10 medium plus 10% (v/v) OADC (Becton Dickinson) containing compound 1 and 13 at 5X or 10X MIC_{99}. Resistance was confirmed by measuring MIC_{99} on solid medium – defined as minimum concentration that inhibits 99% of CFU (34). Genome sequencing and identification of polymorphisms were essentially carried out as described by by Ioerger *et al* (14). In order to determine the rate of spontaneous resistant mutants, *M. tuberculosis* H37RV was grown at 37°C in fresh Middlebrook 7H9-ADC-Tween 80 to mid-exponential phase and then diluted in fresh Middlebrook 7H9-ADC-Tween 80 to $5x10^8$ CFU/mL. Middlebrook 7H10-OADC plates with 4 and 10-fold MIC of each compound were inoculated with 10^8, 10^7, 10^6, and 10^5 CFU/plate, and the plates were incubated at 37°C for 3 to 4 weeks. The frequency of appearance of resistant mutants was calculated, and isolated colonies were restreaked onto Middlebrook 7H10-OADC agar containing the drugs and on plates without the drug.

Time-kill *assay*. Compounds were added at 20xMIC to a 10 mL exponential culture of *M. tuberculosis* H37Rv (~$5x10^5$ cfu/mL) in Middlebrook 7H9 with 10% (v/v) OADC and 0.05% (v/v) Tween-80. At specified time points, aliquots of cultures were withdrawn, serially diluted and plated on solid culture medium. Plates were then incubated at 37°C and CFU were counted after 3 to 4 weeks.

***In vitro* cytotoxicity assay.** Vero epithelial cells (from African green monkey; ATCC CCL-81) were cultured in Dulbecco's modified Eagle's medium (DMEM) supplemented with 10% fetal bovine serum (FBS) and maintained in a humidified incubator (37^0C, 5% CO_2). Cells were dislodged with a cell scraper, collected by centrifugation, resuspended in fresh medium at ~10^6 cells/mL, dispensed into 96-well microtitre plates (100mL/well) and incubated for

168 18h at 37^0C. Two-fold serial dilutions of test compounds (800–0.4 mg/L) in DMEM with
169 FBS were subsequently added and cells incubated for another 72h. From triplicate studies,
170 the cytopathic effects of compounds were evaluated colorimetrically using the MTT cell
171 proliferation assay (ATCC). IC_{50} data were obtained from dose–response curves plotted using
172 Graphpad prism 5.

173 **Mitochondrial protein synthesis assay.** Human liver carcinoma derived HepG2 cell line
174 was obtained from the ATCC (HB-8065). HepG2 cells were grown in Dulbecco's Modified
175 Eagle's medium containing 10% Fetal Calf Serum, 1 mM sodium pyruvate, 0.1 mM non
176 essential amino acids and 50 units/mL penicillin-streptomycin at 37^0C with 5% CO_2. HepG2
177 cells were seeded in 96-well plates at 3000 cells/200 µL/well in cell culture medium. Cells
178 were then grown in the presence of the compounds at 37 °C in 10% CO_2 for 7 days in at least
179 duplicate concentrations, with the medium and compounds being replaced on the fourth day.
180 After 7 days the levels of SDHA and COX1 were determined by using the MitoSciencesTM
181 In-Cell ELISA kit. Janus Green staining was used to determined cell viability after 7 days
182 (In-cell ELISA kit, cat # MS643).

183 **Mouse pharmacokinetic analysis.** The studies were conducted using female CD-1 for
184 compounds 1, 11 and 12, while BALB/C mice were used for compound 13. Mice body
185 weights were 19-28 g and on the morning of dosing, mice were split randomly into 3 dosing
186 groups to receive test article by either tail-vein injection (IV) or oral gavage (PO). After
187 dosing, blood samples were collected via cardiac puncture at specific time points (n=3
188 mice/time point) through 24 hours (K_2EDTA as anticoagulant) and processed for plasma.
189 Antibiotic concentrations in the plasma samples were analysed by LC/MS/MS. The
190 LC/MS/MS analysis was conducted using analyte/internal standard peak area methods. The
191 minternal standard was AN3365 (13) and the instrument was a API4000 QTRAP (AB Sciex).
192 The limit of quantitation (LOQ) was 1 or 2 ng/mL. Pharmacokinetic analyses of the mean
193 plasma concentration-time profiles were performed using WinNonlin Pro version 5.2. A
194 compartmental model was used for the IV data and non-compartmental model for PO data.
195 The time-concentration curve after an IV dose showed a bi-exponential decline with first-
196 order elimination. Compound 1 and 13 were formulated in saline (0.9% w/v NaCl) at 7.5
197 mg/mL and the pH adjusted to >5 by the addition of NaOH. Compound 11 was formulated
198 to 6.5 mg/mL in Water/Dimethylacetamide/EtOH (76/19/5) and the pH adjusted to >5 by the
199 addition of NaOH. Compound 12 was formulated to 7.5 mg/mL in PEG300/PG/water
200 (55/25/20) and the pH adjusted to >5 by the addition of NaOH.

Mouse plasma protein binding determination. Compounds were added to 1.5-mL aliquots of mouse plasma and plasma ultrafiltrate to the following concentrations: 1 µg/mL and 10 µg/mL, and then incubated in a shaking water-bath at 37 °C for 15 minutes. Both samples were treated similarly and a 0.5-mL aliquot was removed from each tube and added to the filter reservoir of the Microcon® centrifugal filter devices (Ultracel YM-30, MWCO=30K Da, Bedford, MA). The devices were centrifuged at 1000 x *g* for 10 minutes and 100 µL of filtrate was transferred to the 96-well plate and diluted 5-fold. Ten-µL volumes of the samples were injected and analyzed with the LC/MS/MS system. All samples were analysed in duplicate. Quantitation was based on peak area ratio of analyte over internal standard and all integrations were performed with peak areas using Analyst version 1.4.1 (Applied Biosystems, Foster City, CA 94404, USA). Plasma protein binding was calculated, based on the following equation:

$$\text{Plasma Protein Binding (\%)} = \frac{(PeakArea^{Spiked}_{PlasmaUltrafiltrate} - PeakArea^{Filtrate}_{Plasma})}{PeakArea^{Spiked}_{PlasmaUltrafiltrate}} * 100$$

Murine model of acute TB infection using C57/BL GKO IFNγ mice. Eight- to 10-week-old female specific-pathogen-free C57BL/6-Ifngtm1ts mice (IFNγ gene-disrupted [GKO] mice) were purchased from Jackson Laboratories, Bar Harbor, ME. The mice were infected via a low-dose aerosol exposure with *M. tuberculosis* Erdman in a Middlebrook aerosol generation device (Glas-Col Inc., Terre Haute, IN) as described previously (18). One day post-aerosol, three mice were sacrificed to verify the uptake of 50 to 100 CFU of bacteria per mouse. Each treatment group consisted of five mice and treatment was started 10-13 days post-infection and continued for nine or fourteen consecutive days. Five infected mice were sacrificed at the start of treatment as pretreatment controls. Drugs were administered daily by oral gavage. Lungs were harvested 24 hours after the last administration and all lung lobes were aseptically removed, homogenized and frozen. Homogenates were plated on 10% OADC-7H11 medium for 21 days at 37ºC. All animal studies strictly adhered to the protocols and regulations approved by their respective Animal Care and Use Committees of University of Illinois at Chicago and Colorado State University.

Murine model of acute and chronic TB infection using C57/BL6J mice. Specific pathogen-free, 8-10 week-old female C57BL/6 mice were purchased from Harlan Laboratories and were allowed to acclimate for one week. The experimental design for the acute assay has been previously described (30). In brief, for the acute assay, mice were intratracheally infected with 100,000 CFU/mouse (*M. tuberculosis* H37Rv strain). Products

233 were administered for 8 consecutive days starting one day after infection. For the chronic
234 assay, mice were intratracheally infected with 100 CFU/mouse and the products administered
235 daily (7 days a week) for 8 consecutive weeks starting 6 weeks after infection. Lungs were
236 harvested 24 hours after the last administration. All lung lobes were aseptically removed,
237 homogenized and frozen. Homogenates were plated on 10% OADC-7H11 medium and
238 incubated for 21 days at 37ºC. The viable colony forming units were converted to logarithms,
239 which were then evaluated by a one-way analysis of variance, followed by a multiple-
240 comparison analysis of variance by a one-way Tukey test (SigmaStat software program).
241 Differences were considered significant at the 95% level of confidence. All animal studies
242 were ethically reviewed and carried out in accordance with European Directive 2010/63/EU
243 and the GSK Policy on the Care, Welfare and Treatment of Animals.
244 **Murine model of chronic TB infection using BALB/c mice.** Six- to 8-week-old female
245 specific-pathogen-free immunocompetent BALB/c mice (Charles River, Wilmington, MA)
246 were infected via a low-dose aerosol exposure to *M. tuberculosis* Erdman as described (18).
247 One day post-aerosol, three mice from each run were sacrificed to verify the uptake of 50 to
248 100 CFU of bacteria per mouse. Each group consisted of five to six mice at each time point.
249 Treatment was started 3 weeks post-infection and continued for 12 weeks. Five infected mice
250 were sacrifice at the start of treatment as pretreatment controls. Drugs were administered 5
251 days per week by oral gavage, for four weeks. Lungs were harvested 72 hours after the last
252 administration. All lung lobes were aseptically removed, homogenized and frozen.
253 Homogenates were plated on 10% OADC-7H11 medium and incubated for 21 days at 37ºC.
254 All animal studies strictly adhered to the protocols and regulations approved by Colorado
255 State University's Animal Care and Use Committee.
256

RESULTS AND DISCUSSION

Discovery of antitubercular LeuRS inhibitors. A focus library of 20 benzoxaboroles was initially screened against *M. tuberculosis* H37Rv, which yielded AN3016 and AN3017 with minimal inhibitory concentration (MIC) of 1 µg/mL and 1.8 µg/mL and LeuRS half-maximal inhibitory concentration (IC_{50}) of 3.5 µM and 0.64 µM, respectively (Fig. 1). When we combined both the 3-aminomethyl and the 7-ethoxy substitutions in one moiety, compound 1, it gave significantly better activity with a LeuRS IC_{50} of 0.28 µM and an MIC of 0.26 µg/mL (Fig. 1). To confirm that compound 1 was targeting LeuRS in the cell, we obtained resistant mutants of *M. tuberculosis* H37Rv and *Mycobacterium smegmatis* ATCC 700084. The *leuS* gene, which codes for LeuRS, was sequenced from selected resistant mutants and mutations were found in both organisms, which was consistent for an OBORT LeuRS inhibitor (Fig. 2 and Table 1). Therefore, we progressed compound 1 into an *in vivo* mouse pharmacokinetic study to determine suitability for testing in an acute TB mouse model. Compound 1 was dosed by oral administration (PO) at 30 mg/kg, which yielded an area under the curve over 24 hrs (AUC_{0-24}) of 15 h*µg/mL with a maximum plasma level (C_{max}) of 4.33 µg/mL and oral bioavailability of 55% (data not shown). Since the existing *in vivo* efficacy mouse model used *M. tuberculosis* Erdman and not *M. tuberculosis* H37Rv, the MIC of compound 1 was confirmed against the Erdman strain as well as some drug-resistant isolates (Table 2). The *M. tuberculosis* Erdman MIC value was 0.127 µg/mL, which was not affected by resistance mechanisms to rifampin, isoniazid or streptomycin. Compound 1 was then tested in a BALB/c acute model of TB dosed at 100 mg/kg twice-a-day (BID) for 3 weeks with weekend drug holidays. The control drug, PA-824 (Pretomanid) (35), was dosed at 100 mg/kg once-a-day (QD), which gave a 1.9 $\log_{10}$ reduction in colony forming units (CFU) from mouse lungs compared to only a 0.4 $\log_{10}$ reduction in CFU for compound 1 (data not shown). Therefore, we separated the two enantiomers in compound 1 by chiral HPLC and determined their activities (Fig. 1). The active enantiomer was the (*S*)-isomer, compound 2, which had a LeuRS IC_{50} of 0.13 µM and an MIC of 0.13 µg/mL, while the (*R*)-isomer was barely active with an IC_{50} of 21 µM. The active enantiomer, compound 2, was then tested at 200 mg/kg BID for 9 days in the acute TB model using an IFN-γ gene knock-out (GKO) mouse (17), which showed a 2 $\log_{10}$ reduction in lung CFU and a 1.5 $\log_{10}$ reduction in spleen CFU compared to the control mice (Fig. 3). However, this was not as good as the frontline drug isoniazid (INH), which gave a 2.8 and 3.4 $\log_{10}$ reduction in CFU from lungs and spleen, respectively, when dosed at 25 mg/kg.

290 ***M. tuberculosis* LeuRS inhibitor co-crystalization.** In order to improve potency we
291 performed structural and biophysical studies to understand the binding mode of these novel
292 3-aminomethyl benzoxaboroles to *M. tuberculosis* LeuRS. Crystallization trials with different
293 editing domain constructs of *M. tuberculosis* LeuRS were attempted in the presence of
294 compound 2 with either AMP or longer nucleotides such as CytAde or CytCytAde, which
295 might act as surrogates for the 3′-end of the tRNA acceptor stem (32). An editing domain
296 construct encompassing residues G309-I513 gave co-crystals with compound 2 and AMP that
297 diffracted to 1.3 Å resolution, which permitted structure determination (Fig. 4A, 4B and
298 Table S1). Compound 2 forms a bidentate covalent adduct with AMP (Fig. 4B), which
299 mimics Ade76 of the tRNA acceptor end (13, 19, 26). The amino acid residues, T336-T337,
300 of the threonine-rich region provides multiple H-bonding interactions to the covalent adduct,
301 and L432 and Y435 of the AMP binding loop have extensive H-bonding and hydrophobic
302 contacts with AMP (Fig. 4B). In addition, the amino group of compound 2 makes three key
303 interactions with the carboxylic acid side chains of D447 and D450 and the carbonyl of
304 M441. The 7-ethoxy enables not only a new interaction to R449 but also packs with the
305 Ade76 ribose, thus further stabilizing the boron-tRNA adduct (Fig. 4B). Superposition of the
306 compound 2 adduct bound structure with that of the *E. coli* LeuRS editing domain with
307 methionine bound (20) shows that the 3-aminomethyl benzoxaborole moiety occupies the
308 same position as the non-cognate amino acid (Fig. 4C). Although this moiety mimics the
309 interactions established by the amino and the oxygen carbonyl groups of methionine, it lacks
310 atoms at the positions of the S^{δ}-C^{ε} atoms of methionine (Fig. 4C), which suggests that there is
311 additional space to make further interactions.
312 **SAR of potent antituberculars.** Several derivatives were synthesized with different
313 substitutions at position 4 as well as at positions 5 and 6 to explore this hypothesis (Fig. 1).
314 The halogen substitutions 5-Cl (compound 5) and 6-F (compound 7) were not well tolerated
315 with LeuRS IC_{50} values worse than the original compound 1 and MIC values of 1.1 µg/mL or
316 greater. The most potent analogs were compounds with halogen substitutions at position 4,
317 bromo (compound 11), chloro (compound 4) and fluoro (compound 6), which improved MIC
318 values more than 5-fold over compound 1 (Fig. 1). The phenyl (compound 10) substitution
319 was not tolerated with LeuRS IC_{50} values of 28 µM (Fig. 1). However, it must be noted that
320 the significant improvements in MIC values for compounds 4, 6 and 11 were not fully
321 reflected in their IC_{50} values as determined using an aminoacylation assay with *M.*
322 *tuberculosis* LeuRS, which could be due to the way that OBORT inhibitors indirectly inhibit

Antimicrobial Agents and Chemotherapy

323 aminoacylation by preventing Ade76 binding to the aminoacylation active site (29). We
324 therefore decided to measure the direct binding of the compounds to the editing domain using
325 isothermal titration calorimetry (ITC) and found that the 4-Cl and 4-Br substitutions
326 significantly enhanced the affinity of the compounds to the *M. tuberculosis* LeuRS editing
327 domain (Table 3). The increased affinity is due to a significant gain in the enthalpic
328 contribution (3.1-4.5 Kcal mol^{-1}), which is consistent with additional favourable interactions
329 being established by the halogen atoms in the editing site. To confirm whole cell activity was
330 derived from inhibition of LeuRS we selected 6 *M. tuberculosis* mutants resistant to
331 compound 13 and sequenced their *leuS* gene, while two additional mutants were selected for
332 whole genome sequencing. All 8 resistant mutants had SNP in their *leuS* genes and the
333 mutations were located in the editing domain as expected for OBORT LeuRS inhibitors (13,
334 24, 29) (Table S2). To further explore interactions at 4-position, we co-crystallised
335 compounds with 4-Cl and 4-Br substitutions in the presence of AMP and solved the
336 structures of the ternary complexes at 1.45 and 1.47 Å resolution, respectively (Table S1, Fig.
337 S1). The structures showed that the halogenated compounds bind to the editing site without
338 major structural changes and as predicted, the 4-Cl/Br atoms now occupy the position of the
339 sulphur in bound methionine (Fig. S2A) allowing van der Waals interactions with the
340 neighbouring protein atoms (Fig. S2B). These results confirmed the importance of the size
341 and nature of the substitution at position 4, and agreed well with the *in vitro* activities and
342 thermodynamic analysis (Fig. S2C).

343 We selected the three most potent compounds, 11, 12 and 13, for *in vivo* murine
344 pharmacokinetic analysis and we dosed mice both intravenously (IV) and orally (PO). All
345 three compounds showed improvements in plasma exposure as measured by AUC after oral
346 administration over compound 2 (Table 4). Therefore, we tested them in a GKO mouse
347 model of acute TB, which showed all to be very efficacious with the racemate compound 11
348 having similar efficacy to isoniazid (Fig. 5AB). In a chronic TB BALB/c mouse model, all
349 compounds showed good efficacy (Fig. 5C) with compound 14, the (*S*)-isomer of compound
350 11, being the most potent. In addition, we observed that compounds 13 and 14 did not show
351 any cross-resistance against multidrug-resistant isolates (Table S3).

352 **Inhibition of mitochondrial protein synthesis.** Although protein synthesis inhibitors are
353 validated TB drugs they are associated with some safety concerns, for example
354 myelosuppression and neuropathy observed with linezolid (16) and deafness induced by
355 aminoglycosides (12). The similarity between the bacterial and mitochondrial protein
356 synthesis machinery (2) and their subsequent inhibition of mitochondrial protein synthesis is

357 thought to drive these toxicities. Therefore, we tested the ability of compound 14 and some
358 close analogues to inhibit mitochondrial protein synthesis in the human liver carcinoma cell
359 line HepG2 (Table 5). The ribosomal protein synthesis inhibitors linezolid, chloramphenicol
360 and doxycycline inhibited the synthesis of the mitochondrial derived COX1 protein with EC_{50}
361 values of between 23 and 31 μM, while erythromycin and compounds 12, 13 and 14 had
362 EC_{50} values of >150 μM. Although this could be due to poor mitochondrial penetration, it is
363 interesting to note that human mitochondrial LeuRS is known to be editing defective as it
364 lacks key conserved amino acid residues in the AMP binding loop and amine binding pocket
365 (21).

366 **Compound 14 *in vitro* and *in vivo* activity.** Since the racemate 11 had similar activity to
367 isoniazid, which is an *in vitro* bactericidal compound (8), in the acute GKO mouse model
368 (Fig. 5B**)** we tested the enantiomer pure compound 14 for *in vitro* bactericidal activity over
369 14 days at 20-fold its MIC (Fig. 6**)**. The profile for compound 14 was very similar to the
370 bacteriostatic protein synthesis inhibitor, linezolid, which was different from moxifloxacin a
371 known bactericidal compound (33). Therefore, further tests of compound 14 in a murine
372 chronic TB model (Fig. 7) were performed in parallel with the protein synthesis inhibitor
373 linezolid. Compound 14 at 30 mg/kg QD showed good efficacy resulting in a 2.4 $\log_{10}$
374 reduction in CFU compared with a 2.6 $\log_{10}$ reduction in CFU for 100 mg/kg QD of linezolid.
375 In order to establish the optimal dosing regimen for compound 14 we tested it in the acute TB
376 murine model and compared the efficacy from the following dosing regimes, BID, QD and
377 q48h (Fig. 8). Similar to results in the chronic model, compound 14 was more active at lower
378 doses than linezolid and dosing every other day (q48h) was as efficacious as QD or even
379 BID, which suggests that the preliminary pharmacodynamic driver for efficacy was
380 AUC/MIC.

381 **Resistance and LeuRS inhibitors.** Emergence of resistance during streptomycin
382 monotherapy (1) and its noted reduction by the addition of p-aminosalicyclic acid (11, 23)
383 lead to the paradigm of combination TB drug therapy. The current core TB regimen calls for
384 a four-drug combination of isoniazid, rifampin, ethambutol and pyrazinamide. Although
385 compound 14 has a lower *in vitro* resistance frequency than isoniazid (Supplementary Table
386 7), the emergence of resistance to epetraborole (GSK2251052/AN3365), another 3-
387 aminomethylbenzoxaborole LeuRS inhibitor, in a minority of patients in a complicated
388 urinary tract infection trial might suggest some caution (24). However, the addition of
389 trimethoprim to rifampicin, which has a similar resistance problem, in an urinary tract
390 infection trial demonstrated the benefit of combination therapy in overcoming emergence of

391 rifampin-resistant strains (27). This suggests that the risk from emergence of resistance to
392 OBORT LeuRS inhibitors will likely be mitigated when used in combination therapy.
393 **Beneficial properties.** Since combination therapy necessitates a larger armamentarium than
394 regular monotherapy, the demonstration for the first time that an oral AARS inhibitor can be
395 a potent antitubercular adds a potential new tool to fight TB, which is timely noting the recent
396 onset of TDR-TB. In addition, the combination of low plasma protein binding, molecular
397 weight (207-285) and $\log D_{7.4}$ (-0.04-0.76), like the frontline TB drugs isoniazid,
398 pyrazinamide and ethambutol, suggests that this novel chemical class deserves further
399 optimisation and hopefully progression into clinical trials.
400

401 **REFERENCES**

402 1. 1948. Streptomycin treatment of pulmonary tuberculosis. British medical journal
403 **2:**769-782.

404 2. **Benne, R., and P. Sloof.** 1987. Evolution of the mitochondrial protein synthetic
405 machinery. Bio Systems **21:**51-68.

406 3. **C.C.P.N.** 1994. The CCP4 suite: programs for protein crystallography. Acta
407 Crystallogr D **D50:**760-763.

408 4. **Chen, V. B., W. B. Arendall, 3rd, J. J. Headd, D. A. Keedy, R. M. Immormino,**
409 **G. J. Kapral, L. W. Murray, J. S. Richardson, and D. C. Richardson.** 2010.
410 MolProbity: all-atom structure validation for macromolecular crystallography. Acta
411 Crystallogr D Biol Crystallogr **66:**12-21.

412 5. **Cheng, A. F., W. W. Yew, E. W. Chan, M. L. Chin, M. M. Hui, and R. C. Chan.**
413 2004. Multiplex PCR amplimer conformation analysis for rapid detection of gyrA
414 mutations in fluoroquinolone-resistant *Mycobacterium tuberculosis* clinical isolates.
415 Antimicrobial agents and chemotherapy **48:**596-601.

416 6. **Collins, L., and S. G. Franzblau.** 1997. Microplate alamar blue assay versus
417 BACTEC 460 system for high-throughput screening of compounds against
418 *Mycobacterium tuberculosis* and *Mycobacterium avium*. Antimicrobial agents and
419 chemotherapy **41:**1004-1009.

420 7. **Cusack, S., A. Yaremchuk, and M. Tukalo.** 2000. The 2 A crystal structure of
421 leucyl-tRNA synthetase and its complex with a leucyl-adenylate analogue. The
422 EMBO journal **19:**2351-2361.

423 8. **de Steenwinkel, J. E., G. J. de Knegt, M. T. ten Kate, A. van Belkum, H. A.**
424 **Verbrugh, K. Kremer, D. van Soolingen, and I. A. Bakker-Woudenberg.** 2010.
425 Time-kill kinetics of anti-tuberculosis drugs, and emergence of resistance, in relation

to metabolic activity of *Mycobacterium tuberculosis*. The Journal of antimicrobial chemotherapy **65:**2582-2589.

9. **Emsley, P., and K. Cowtan.** 2004. Coot: model-building tools for molecular graphics. Acta Crystallogr D Biol Crystallogr **60:**2126-2132.

10. **Englisch, S., U. Englisch, F. von der Haar, and F. Cramer.** 1986. The proofreading of hydroxy analogues of leucine and isoleucine by leucyl-tRNA synthetases from *E. coli* and yeast. Nucleic acids research **14:**7529-7539.

11. **Graessle, O. E., and J. J. Pietrowski.** 1949. The *in vitro* effect of para-aminosalicylic acid (PAS) in preventing acquired resistance to streptomycin by *Mycobacterium tuberculosis*. Journal of bacteriology **57:**459-464.

12. **Hamasaki, K., and R. R. Rando.** 1997. Specific binding of aminoglycosides to a human rRNA construct based on a DNA polymorphism which causes aminoglycoside-induced deafness. Biochemistry **36:**12323-12328.

13. **Hernandez, V., T. Crepin, A. Palencia, S. Cusack, T. Akama, S. J. Baker, W. Bu, L. Feng, Y. R. Freund, L. Liu, M. Meewan, M. Mohan, W. Mao, F. L. Rock, H. Sexton, A. Sheoran, Y. Zhang, Y. K. Zhang, Y. Zhou, J. A. Nieman, M. R. Anugula, M. Keramane el, K. Savariraj, D. S. Reddy, R. Sharma, R. Subedi, R. Singh, A. O'Leary, N. L. Simon, P. L. De Marsh, S. Mushtaq, M. Warner, D. M. Livermore, M. R. Alley, and J. J. Plattner.** 2013. Discovery of a novel class of boron-based antibacterials with activity against Gram-negative bacteria. Antimicrobial agents and chemotherapy **57:**1394-1403.

14. **Ioerger, T. R., T. O'Malley, R. Liao, K. M. Guinn, M. J. Hickey, N. Mohaideen, K. C. Murphy, H. I. Boshoff, V. Mizrahi, E. J. Rubin, C. M. Sassetti, C. E. Barry, 3rd, D. R. Sherman, T. Parish, and J. C. Sacchettini.** 2013. Identification of new

drug targets and resistance mechanisms in *Mycobacterium tuberculosis*. PloS one **8:**e75245.

15. **Kabsch, W.** 1993. Automatic processing of rotation diffraction data from crystals of initially unknown symmetry and cell constants. J. Appl. Cryst. **26:**795-800.

16. **Lee, M., J. Lee, M. W. Carroll, H. Choi, S. Min, T. Song, L. E. Via, L. C. Goldfeder, E. Kang, B. Jin, H. Park, H. Kwak, H. Kim, H. S. Jeon, I. Jeong, J. S. Joh, R. Y. Chen, K. N. Olivier, P. A. Shaw, D. Follmann, S. D. Song, J. K. Lee, D. Lee, C. T. Kim, V. Dartois, S. K. Park, S. N. Cho, and C. E. Barry, 3rd.** 2012. Linezolid for treatment of chronic extensively drug-resistant tuberculosis. The New England journal of medicine **367:**1508-1518.

17. **Lenaerts, A. J., V. Gruppo, J. V. Brooks, and I. M. Orme.** 2003. Rapid *in vivo* screening of experimental drugs for tuberculosis using gamma interferon gene-disrupted mice. Antimicrobial agents and chemotherapy **47:**783-785.

18. **Lenaerts, A. J., V. Gruppo, K. S. Marietta, C. M. Johnson, D. K. Driscoll, N. M. Tompkins, J. D. Rose, R. C. Reynolds, and I. M. Orme.** 2005. Preclinical testing of the nitroimidazopyran PA-824 for activity against *Mycobacterium tuberculosis* in a series of *in vitro* and *in vivo* models. Antimicrobial agents and chemotherapy **49:**2294-2301.

19. **Lincecum, T. L., Jr., M. Tukalo, A. Yaremchuk, R. S. Mursinna, A. M. Williams, B. S. Sproat, W. Van Den Eynde, A. Link, S. Van Calenbergh, M. Grotli, S. A. Martinis, and S. Cusack.** 2003. Structural and mechanistic basis of pre- and posttransfer editing by leucyl-tRNA synthetase. Molecular cell **11:**951-963.

20. **Liu, Y., J. Liao, B. Zhu, E. D. Wang, and J. Ding.** 2006. Crystal structures of the editing domain of *Escherichia coli* leucyl-tRNA synthetase and its complexes with

474 Met and Ile reveal a lock-and-key mechanism for amino acid discrimination. The
475 Biochemical journal **394:**399-407.

476 21. **Lue, S. W., and S. O. Kelley.** 2005. An aminoacyl-tRNA synthetase with a defunct
477 editing site. Biochemistry **44:**3010-3016.

478 22. **McCoy, A. J., R. W. Grosse-Kunstleve, L. C. Storoni, and R. J. Read.** 2005.
479 Likelihood-enhanced fast translation functions. Acta Crystallogr D Biol Crystallogr
480 **61:**458-464.

481 23. **Nagley, M. M.** 1950. The combined use of para-aminosalicylic acid (PAS) and
482 streptomycin in pulmonary tuberculosis. Tubercle **31:**151-155.

483 24. **O'Dwyer, K., A. T. Spivak, K. Ingraham, S. Min, D. J. Holmes, C. Jakielaszek, S.**
484 **Rittenhouse, A. L. Kwan, G. P. Livi, G. Sathe, E. Thomas, S. Van Horn, L. A.**
485 **Miller, M. Twynholm, J. Tomayko, M. Dalessandro, M. Caltabiano, N. E.**
486 **Scangarella-Oman, and J. R. Brown.** 2015. Bacterial resistance to leucyl-tRNA
487 synthetase inhibitor GSK2251052 develops during treatment of complicated urinary
488 tract infections. Antimicrobial agents and chemotherapy **59:**289-298.

489 25. **Ollinger, J., M. A. Bailey, G. C. Moraski, A. Casey, S. Florio, T. Alling, M. J.**
490 **Miller, and T. Parish.** 2013. A dual read-out assay to evaluate the potency of
491 compounds active against *Mycobacterium tuberculosis*. PloS one **8:**e60531.

492 26. **Palencia, A., T. Crepin, M. T. Vu, T. L. Lincecum, Jr., S. A. Martinis, and S.**
493 **Cusack.** 2012. Structural dynamics of the aminoacylation and proofreading functional
494 cycle of bacterial leucyl-tRNA synthetase. Nature structural & molecular biology
495 **19:**677-684.

496 27. **Palminteri, R., and D. Sassella.** 1979. Double-blind multicenter trial of a rifampicin-
497 trimethoprim combination and rifampicin alone in urinary tract infections.
498 Chemotherapy **25:**181-188.

28. **Perrakis, A., R. Morris, and V. S. Lamzin.** 1999. Automated protein model building combined with iterative structure refinement. Nat Struct Biol **6:**458-463.

29. **Rock, F. L., Mao, W., A. Yaremchuk, M. Tukalo, T. Crepin, H. Zhou, Y. K. Zhang, V. Hernandez, T. Akama, S. J. Baker, J. J. Plattner, L. Shapiro, S. A. Martinis, S. J. Benkovic, S. Cusack, and M. R. Alley.** 2007. An antifungal agent inhibits an aminoacyl-tRNA synthetase by trapping tRNA in the editing site. Science **316:**1759-1761.

30. **Rullas, J., J. I. Garcia, M. Beltran, P. J. Cardona, N. Caceres, J. F. Garcia-Bustos, and I. Angulo-Barturen.** 2010. Fast standardized therapeutic-efficacy assay for drug discovery against tuberculosis. Antimicrobial agents and chemotherapy **54:**2262-2264.

31. **Sassanfar, M., J. E. Kranz, P. Gallant, P. Schimmel, and K. Shiba.** 1996. A eubacterial *Mycobacterium tuberculosis* tRNA synthetase is eukaryote-like and resistant to a eubacterial-specific antisynthetase drug. Biochemistry **35:**9995-10003.

32. **Seiradake, E., W. Mao, V. Hernandez, S. J. Baker, J. J. Plattner, M. R. Alley, and S. Cusack.** 2009. Crystal structures of the human and fungal cytosolic leucyl-tRNA synthetase editing domains: A structural basis for the rational design of antifungal benzoxaboroles. Journal of molecular biology **390:**196-207.

33. **Shandil, R. K., R. Jayaram, P. Kaur, S. Gaonkar, B. L. Suresh, B. N. Mahesh, R. Jayashree, V. Nandi, S. Bharath, and V. Balasubramanian.** 2007. Moxifloxacin, ofloxacin, sparfloxacin, and ciprofloxacin against *Mycobacterium tuberculosis*: evaluation of *in vitro* and pharmacodynamic indices that best predict *in vivo* efficacy. Antimicrobial agents and chemotherapy **51:**576-582.

522 34. **Sirgel, F. A., I. J. Wiid, and P. D. van Helden.** 2009. Measuring minimum
523 inhibitory concentrations in mycobacteria. Methods in molecular biology **465:**173-
524 186.
525 35. **Stover, C. K., P. Warrener, D. R. VanDevanter, D. R. Sherman, T. M. Arain, M.**
526 **H. Langhorne, S. W. Anderson, J. A. Towell, Y. Yuan, D. N. McMurray, B. N.**
527 **Kreiswirth, C. E. Barry, and W. R. Baker.** 2000. A small-molecule
528 nitroimidazopyran drug candidate for the treatment of tuberculosis. Nature **405:**962-
529 966.
530 36. **Sutherland, R., R. J. Boon, K. E. Griffin, P. J. Masters, B. Slocombe, and A. R.**
531 **White.** 1985. Antibacterial activity of mupirocin (pseudomonic acid), a new antibiotic
532 for topical use. Antimicrobial agents and chemotherapy **27:**495-498.
533 37. **Vondenhoff, G. H., and A. Van Aerschot.** 2011. Aminoacyl-tRNA synthetase
534 inhibitors as potential antibiotics. European journal of medicinal chemistry **46:**5227-
535 5236.
536 38. **Woese, C. R., G. J. Olsen, M. Ibba, and D. Soll.** 2000. Aminoacyl-tRNA
537 synthetases, the genetic code, and the evolutionary process. Microbiology and
538 molecular biology reviews : MMBR **64:**202-236.

539

ACKNOWLEDGMENTS

The authors would like to thank Dr. Ding Zhou and his team at PharmaResources, Dr. Michael Xu and his team at WuXi AppTec, and Dr. James Nieman and his team at NAEJA Pharmaceuticals for their contributions to medicinal chemistry. The authors thank the staff of the EMBL HTX (high-throughput crystallization) platform within the Grenoble Partnership for Structural Biology (PSB) and of the ESRF-EMBL Joint Structural Biology Group for access to ESRF beamlines. AL acknowledges the NIH/NIAID Contract NO1 AI-95385 (TAACF)) for the efficacy testing in acute and chronic mouse models of infection. We thank James Ahn for technical assistance.

ACCESSION CODES

Atomic coordinates and structure factors for the compound 2, 11 and 13 have been deposited in wwPDB with the following codes, 5AGR, 5AGS, 5AGT.

554 **Table 1. MIC values for compound 1 resistant mutants.**

Organism/Mutant /SNP	**Agar MIC (µg/mL)**	**Organism/Mutant /SNP**	**Liquid MIC (µg/mL)**
M. tuberculosis H37Rv	0.6-1.3	*M. smegmatis* ATCC 700084	1
RM1*leuS* Y435C	21	RM1*leuS*Δ421-462	>256
RM2*leuS* S311L	21	RM2*leuS* A428T	64
RM3*leuS* D450Y	21	RM3*leuS* R435C	8
RM4*leuS* S311L	21	RM4*leuS* A428T	64

555 The residues Y435 and D450 stabilize the adduct formed by compound 1 with AMP in the
556 editing site of *M. tuberculosis* LeuRS (Figure 4b). The residue S311, like the equivalent *E.*
557 *coli* LeuRS residue (20), interacts with phosphate of Ade76 thus stabilizing the adduct in the
558 editing site. However, S311 is located at the flexible N-terminal part of our editing domain
559 construct of M. tuberculosis LeuRS and thus is not visible in the crystal structure (Figure 4b).
560 SNP = single nucleotide polymorphism, RM = resistant mutant.

561 **Table 2. Compound 1 MIC (µg/mL) against *M. tuberculosis* Erdman and monoresistant**
562 **isolates compared with known standards**

Strain	Cmp 1	PA-824	RIF	INH	STR
M. tuberculosis Erdman	0.127	0.116	0.018	0.244	0.369
rRIF	0.120	0.128	>4	0.383	0.216
rINH	0.059	≤0.063	0.037	>8	0.202
rSTR	0.113	0.189	0.082	0.344	>16

563 r, resistance to RIF = Rifampin, INH= Isoniazid or STR= Streptomycin

564

565 **Table 3. Thermodynamic analysis of the interaction between *M. tuberculosis* LeuRS and**
566 **benzoxaborole compounds.**

Compound/ parameter	K_d^* (μM)	ΔG_{ap} (Kcal mol^{-1})	ΔH_{ap} (Kcal mol^{-1})	$-T\Delta S_{ap}$ (Kcal mol^{-1})	n
2	3.7	- 7.4	-1.1	-6.3	1.05
13	0.075	-9.7	-4.2	-5.5	1.19
11	0.040	-10.0	-5.5	-4.6	1.02

567 * The error in the thermodynamic binding parameters is about 5% for the apparent binding enthalpy, and 10%
568 for the apparent binding constant and the number of sites (n). Values in the table are the average of at least 2
569 independent experiments.
570

571 **Table 4. Murine Pharmacokinetic Parameters**

*IV	Cmp2	Cmp11	Cmp12	Cmp13	Cmp14
	30	**15**	**30**	**30**	**30**
Cmax (µg/mL) @ 5 min	8.9	18.0	13.7	13.6	17.1
CL (mL/h/kg)	2180	328	1119	582	687
Vss (mL/kg)	2116	968	3805	3142	3221
MRT (h)	2.1	3.0	3.4	5.4	4.7
$AUC_{0-\infty}$ (h*µg/mL)	13.8	45.8	26.8	51.6	43.7
α-$t_{1/2}$ (hr) [%AUC]	0.06[5]	0.09 [2]	0.11 [7]	0.10 [2]	0.05 [5]
β-$t_{1/2}$ (hr) [%AUC]	1.5[95]	2.08 [98]	2.53 [93]	3.83 [98]	3.40 [95]
#PO (mg/kg)	**30**	**30**	**30**	**30**	**30**
Cmax (µg/mL)	3.4	7.2	5.0	6.4	6.3
Tmax (h)	0.50	1.00	1.00	0.25	0.50
AUC_{0-24} (h*µg/mL)	13.2	35.9	23.8	47.5	57.6
Terminal $t_{1/2}$ (h)	1.8	2.7	2.7	3.1	3.6
Bioavailability (%)	96	39	89	92	100
Mouse PPB(%)	6	50	16	23	-

572 *WinNonlin two-compartment analysis iterative weighting.

573 #WinNonlin non-compartment analysis with uniform weighing.

574

575 **Table 5. Mitochondrial protein synthesis inhibition**

Compound	**COX1 EC_{50} (µM)**	**SDHA EC_{50} (µM)**	**Cell Viability EC_{50} (µM)**
Compound 12	>150	39.5 ± 9.2	23.0 ± 1.4
Compound 13	>150	20.5 ± 2.1	80.0 ± 5.7
Compound 14	>150	21.5 ± 6.4	106 ± 37.5
Linezolid	27.3 ± 10.8	>150	>150
Chloramphenicol	31.4 ± 23.2	>150	110 ± 14.1
Doxycycline	23.7 ± 6.4	109 ± 29	118 ± 35.5
Erythromycin	>150	>150	>150

576 COX1 is cytochrome c oxidase, which is a mitochondrial protein that is
577 synthesized by mitochondrial ribosomes. SDHA is subunit A of succinate
578 dehydrogenase complex, which is a mitochondrial protein that is
579 synthesized by cytoplasmic ribosomes. Janus Green staining was used to
580 determined cell viability after 7 days.

581

582 **Table 6. *In vitro* resistance frequency**

Compound	4xMIC	10xMIC
Compound 14	4.6×10^{-6}	3.9×10^{-6}
Isoniazid	ND	1.8×10^{-5}
Moxifloxacin	1.7×10^{-7}	1.1×10^{-8}

583 The MIC values for compound 14, isoniazid and moxifloxacin were
584 determined on Middlebrook 7H10 agar as 0.2, 0.06 and 0.08 µg/mL,
585 respectively.

586

FIGURE LEGENDS

Figure 1. *In vitro* structure-activity relationship. Mtb = *M. tuberculosis*, NT= not tested.

Figure 2. Compound 1 resistant mutants bear mutations in the editing domain of LeuRS. **(A)** Domain map of *M. tuberculosis* LeuRS. **(B)** Amino acid alignment of part of the editing domain of LeuRS from *M. tuberculosis* and *M. smegmatis*, identical residues are colored in blue, non-identical residues are colored in red with arrows indicating where the mutations were found.

Figure 3. *In vivo* efficacy of compound 2 in a murine GKO (C57BL/6-Ifngtm1ts) model of acute TB. Oral treatment was started 15 days (Start) after infection with a low dose aerosol of *M. tuberculosis* Erdman lux and continued for 9 consecutive daily treatments until day 23 when mice were euthanized on day 24 (End). CFU were determined from lungs (black) and spleens (grey) and means from five mice for drug treated groups and 6 mice per group for the untreated controls. $*P < 0.001$ by pairwise multiple comparison procedures (Tukey test) compared to control.

Figure 4. X-ray co-crystal structure of LeuRS with compound 2. **(A)** Crystal structure of *M. tuberculosis* LeuRS editing domain in complex with compound 2 (carbon atoms are colored in green)-AMP (carbon atoms are colored in magenta). Color code is the same throughout all figures with blue for nitrogen, red for oxygen, pink for boron, orange for phosphorus, yellow for sulfur. (**B**) Zoomed view into the editing site of *M. tuberculosis* LeuRS showing the compound 2-AMP adduct and the key residues establishing important hydrogen bonds (red dashed lines) with only the H-bond from the 3-aminomethyl to M441 being omitted for clarity. (**C**) Overlay of the LeuRS editing domain of *M. tuberculosis* and *E. coli* in complex with methionine colored in yellow (PDB: 2AJF). The 3-aminomethyl group of compound 2 mimics the amino group of methionine, including the interaction to the bacterial specific residue D447.

Figure 5. *In vivo* efficacy of compounds 11, 12, 13 and 14 in acute and chronic models of TB infection. **(A)** *In vivo* efficacy in a murine GKO (C57BL/6-Ifngtm1ts) model of acute TB. Compounds were dosed orally daily for 14 days after 10 days infection (Start) with a low dose aerosol of *M. tuberculosis* Erdman. Mean lung CFU were determined from five mice at End. **(B)** *In vivo* efficacy in a murine GKO (C57BL/6-Ifngtm1ts) model of acute TB. Oral treatment was started 13 days after infection (Start) with low dose aerosol of *M. tuberculosis*

618 Erdman lux and continued for 9 consecutive daily treatments until day 21 when mice were
619 sacrificed on day 22 (End). Mean lung CFU were determined from five mice at End. **(c)** *In*
620 *vivo* efficacy in a murine BALB/c model of chronic TB infection. Compounds were dosed
621 orally 5 days a week for 4 weeks after infecting with *M. tuberculosis* Erdman with a low dose
622 aerosol 21 days prior (Start). Lung (black) and spleen (grey) CFU were determined from six
623 mice at End. $^{**}P < 0.01$, $^{*}P < 0.001$ by pairwise multiple comparison procedures (Tukey
624 test) compared to control.

625 **Figure 6.** *M. tuberculosis* H37Rv *in vitro* kill kinetics. Cells were incubated with compounds
626 at 20-fold their MIC values for different times over 14 days in 10 mL of 7H9 10% (v/v) ADC
627 and 0.05% (v/v) Tween 80 medium. The MIC values used in this experiment were as
628 follows, 0.013 µg/mL, 0.6 µg/mL and 0.06 µg/mL for compound 14, linezolid and
629 moxifloxacin, respectively. The mean and the standard deviations of at triplicate cultures of
630 each point are shown.

631 **Figure 7.** Efficacy of compound 14 in a mouse model of chronic TB infection. C57 BL/6J
632 mice were infected with *M. tuberculosis* H37Rv intratracheally (~10^2 CFU) and were dosed
633 once daily for 8 weeks starting 6 weeks after infection. Mice were sacrificed 24 hours after
634 the last drug administration. Every column represents the mean value +/- SD of 7 mice per
635 group for untreated and Linezolid treated groups and 3 mice for Compound 14 treated mice.
636 $^{*}P < 0.001$ by pairwise multiple comparison procedures (Tukey test) compared to control.

637 **Figure 8.** Efficacy of compound 14 in a mouse model of acute TB infection under different
638 dosing regimes of once a day (QD), twice a day (BID) or every other day (q48h). C57 BL/6J
639 mice were infected with *M. tuberculosis* H37Rv intratracheally (~10^5 CFU) and were dosed
640 starting on the following day after infection for 8 days. Only one dose was administered on
641 day 8 under the BID schedule. Mice were sacrificed at least 24 hours after the last drug
642 administration. Every dot represents one mouse data point except for Linezolid (mean of 5
643 mice +/- SD).

FIG. 1

Compound No		IC_{50} (μM) M.tb LeuRS	MIC (μg/mL) M.tb H37RV	EC_{50} (μM) Vero Cells
AN2679		21.3	7.5	NT
AN3016		3.5	1.0	NT
AN3017		0.64	1.8	NT
1		0.28	0.26	>50
2		0.13	0.13	>50
3		21	NT	>50
4		0.09	0.04	>50
5		0.38	1.2	43
6		0.11	0.05	>50
7		0.56	>1.1	>50
8		0.20	0.04	>50
9		0.31	0.29	>50
10		28	17	>50
11		0.11	0.05	>50
12		0.08	0.05	NT
13		0.06	0.02	NT
14		0.08	0.02	NT

FIG. 2

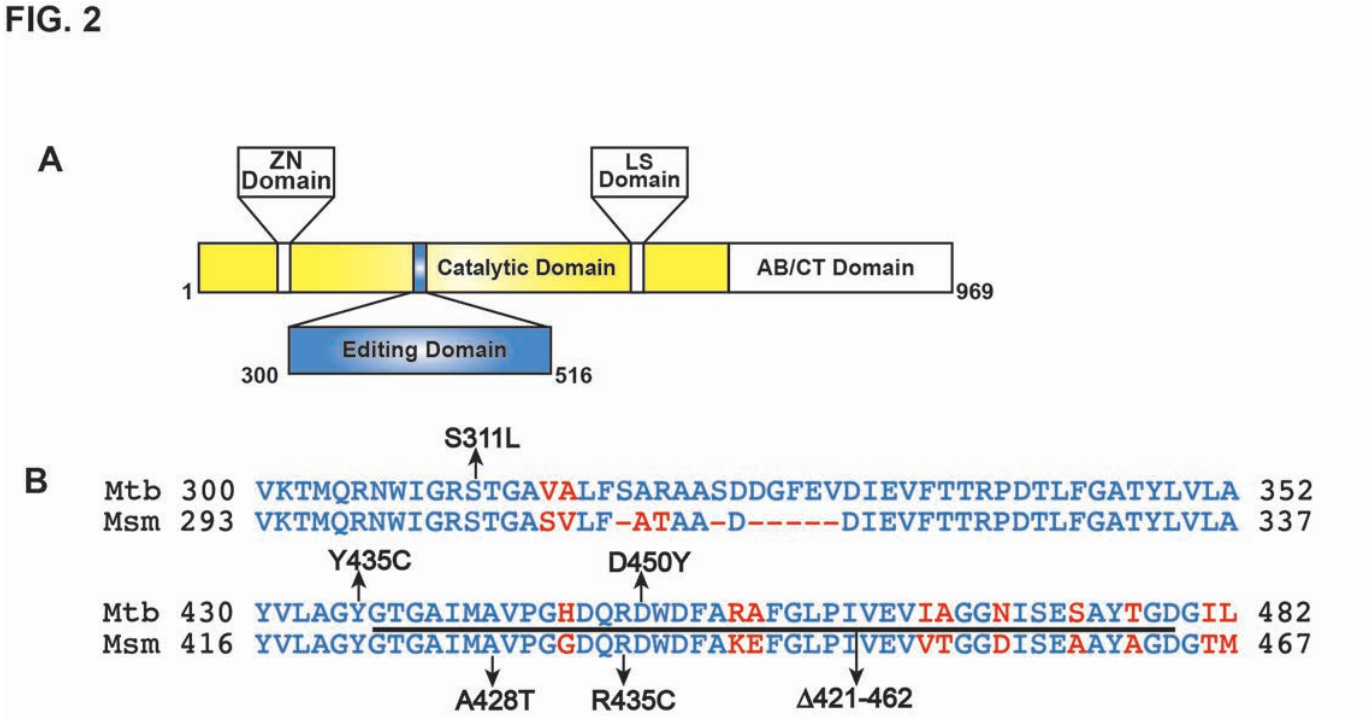

FIG. 3

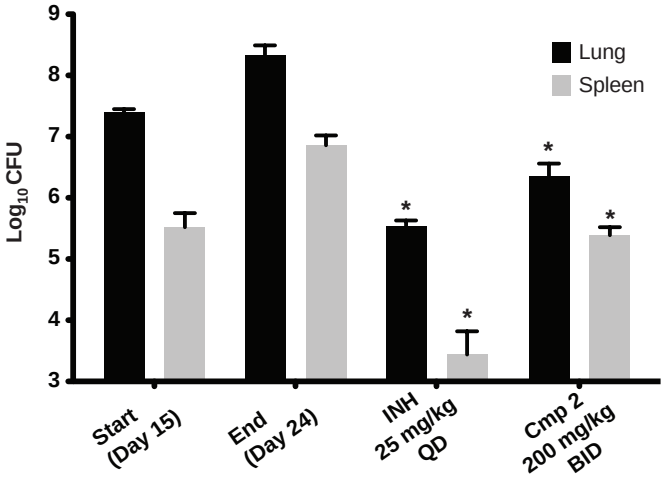

FIG. 4

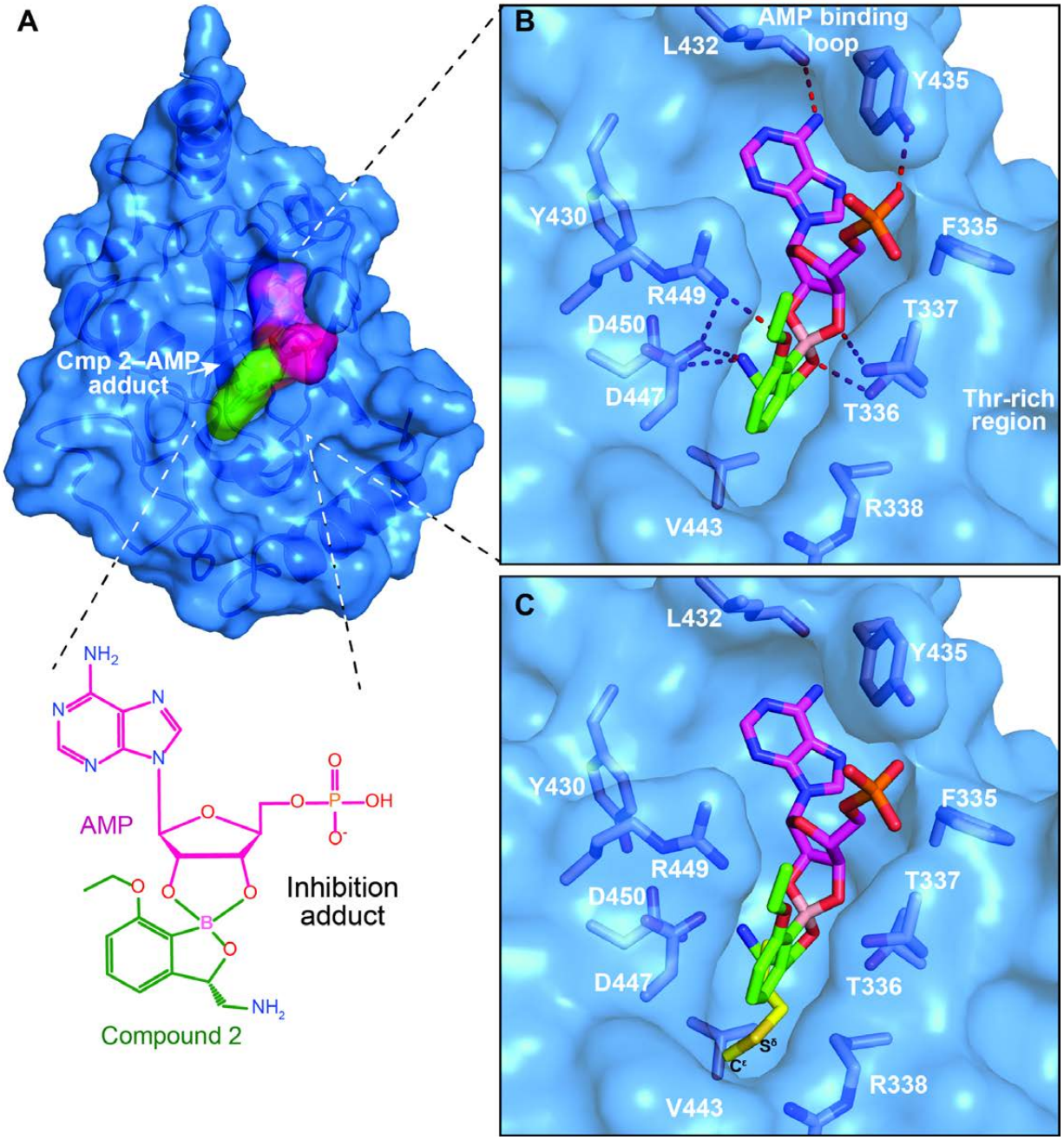

FIG. 5

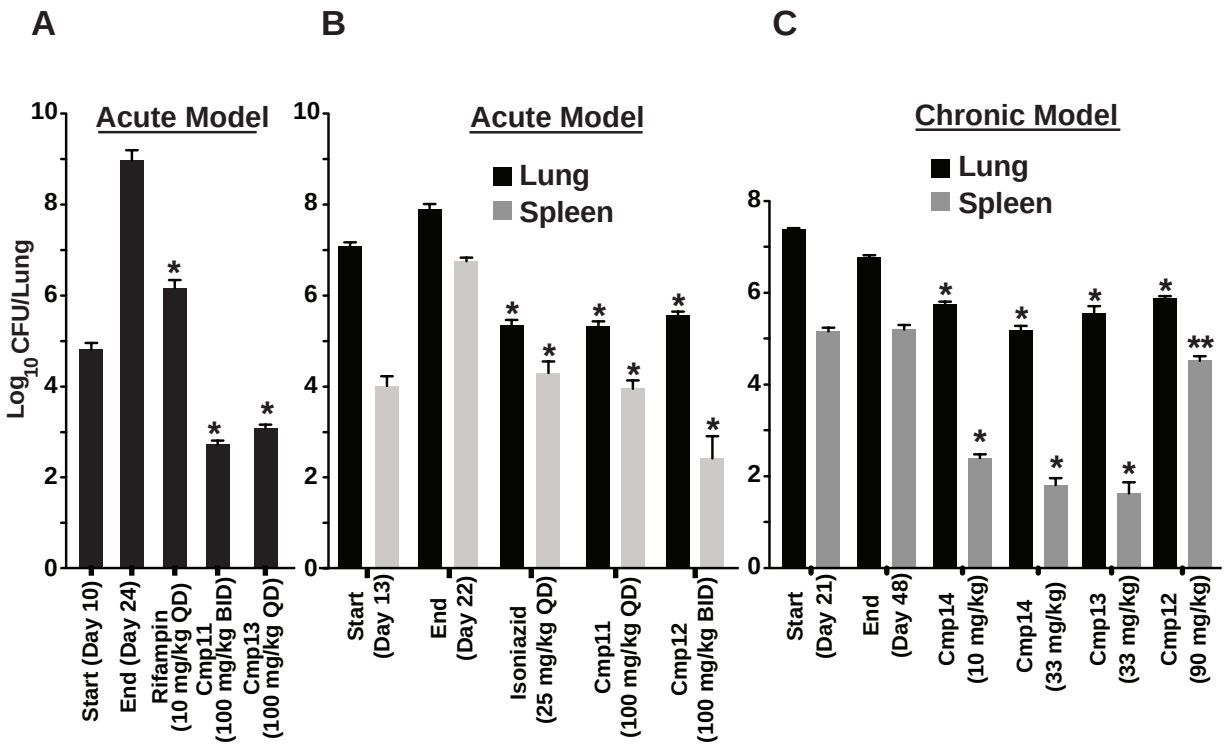

FIG. 6

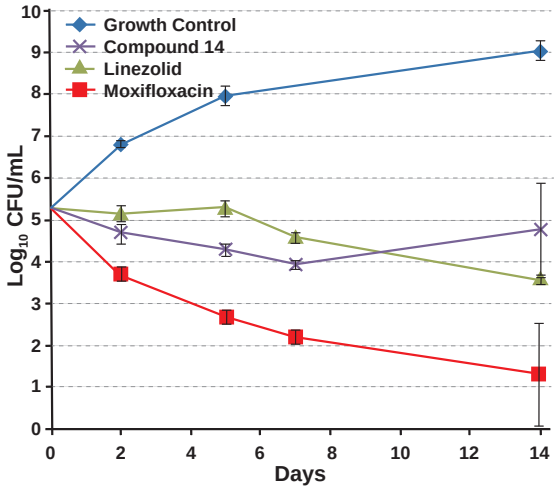

FIG. 7

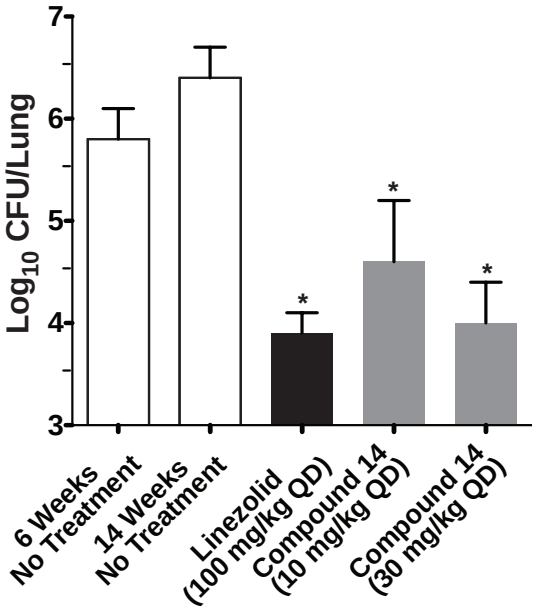

FIG. 8